# *NPHP1* gene-associated nephronophthisis is associated with an occult retinopathy

Johannes Birtel[1,2,3], Georg Spital[4], Marius Book[4], Sandra Habbig[5], Sören Bäumner[5], Vera Riehmer[6], Bodo B. Beck[6,7], David Rosenkranz[8], Hanno J. Bolz[6,8], Mareike Dahmer-Heath[9,10], Philipp Herrmann[3], Jens König[9,10,11] and Peter Charbel Issa[1,2,11]

*[1]Oxford Eye Hospital, Oxford University Hospitals NHS Foundation Trust, Oxford, UK; [2]Nuffield Laboratory of Ophthalmology, Nuffield Department of Clinical Neurosciences, University of Oxford, Oxford, UK; [3]Department of Ophthalmology, University Hospital Bonn, Bonn, Germany; [4]Eye Center at St. Franziskus-Hospital Münster, Münster, Germany; [5]Department of Pediatrics, Faculty of Medicine and University Hospital Cologne, University of Cologne, Cologne, Germany; [6]Institute of Human Genetics, University of Cologne, University Hospital of Cologne, Cologne, Germany; [7]Institute of Human Genetics, Center for Molecular Medicine Cologne, Center for Rare Diseases Cologne, University of Cologne, University Hospital of Cologne, Cologne, Germany; [8]Senckenberg Centre for Human Genetics, Frankfurt, Germany; and [9]Department of General Pediatrics, University Children's Hospital, Münster, Germany*

**Biallelic deletions in the *NPHP1* gene are the most frequent molecular defect of nephronophthisis, a kidney ciliopathy and leading cause of hereditary end-stage kidney disease. Nephrocystin 1, the gene product of *NPHP1*, is also expressed in photoreceptors where it plays an important role in intra-flagellar transport between the inner and outer segments. However, the human retinal phenotype has never been investigated in detail. Here, we characterized retinal features of 16 patients with homozygous deletions of the entire *NPHP1* gene. Retinal assessment included multimodal imaging (optical coherence tomography, fundus autofluorescence) and visual function testing (visual acuity, full-field electroretinography, color vision, visual field). Fifteen patients had a mild retinal phenotype that predominantly affected cones, but with relative sparing of the fovea. Despite a predominant cone dysfunction, night vision problems were an early symptom in some cases. The consistent retinal phenotype on optical coherence tomography images included reduced reflectivity and often a granular appearance of the ellipsoid zone, fading or loss of the interdigitation zone, and mild outer retinal thinning. However, there were usually no obvious structural changes visible upon clinical examination and fundus autofluorescence imaging (occult retinopathy). More advanced retinal degeneration might occur with ageing. An identified additional *CEP290* variant in one patient with a more severe retinal degeneration may indicate a potential role for genetic modifiers, although this requires further investigation. Thus, diagnostic awareness about this distinct retinal phenotype has implications for the differential diagnosis of nephronophthisis and for individual prognosis of visual function.**

**Correspondence:** *Peter Charbel Issa, Oxford Eye Hospital, John Radcliffe Hospital, Oxford OX3 9DU, UK. E-mail: study-enquiry@outlook.com*

[10]MD-H and JK are members of the Neocyst Consortium.

[11]JK and PCI are co-senior authors.

**Received 21 January 2021; revised 4 May 2021; accepted 7 June 2021; published online 19 June 2021**

*Kidney International* (2021) **100,** 1092–1100; https://doi.org/10.1016/j.kint.2021.06.012

KEYWORDS: ciliopathy; genetic modifier; nephronophthisis; *NPHP1*; phenotyping; retinal imaging



Nephronophthisis (NPH) is a leading cause for hereditary end-stage kidney disease in children and young adults.[1] NPH can occur as isolated kidney disease but also as part of multisystem disorders such as Senior-Løken or Joubert syndrome.[2,3] Variants in 20 genes (*NPHP1–NPHP20*), all associated with autosomal recessive inheritance, have been reported to be causative for NPH.[1,4] Because of an often nonspecific clinical presentation, limited genotype-phenotype correlations, and an overlap with other diseases, NPH diagnosis remains challenging.[5,6]

Homozygous deletions encompassing the entire *NPHP1* gene are by far the most common genetic defect found in patients with NPH.[7–11] Nephrocystin 1, the gene product of *NPHP1*, is localized to the primary cilium, and mutations result in an impaired ciliary function.[12] Normal ciliary function is crucial for multiple organ systems, and various systemic disease manifestations are known to be associated with *NPHP1* variants (Figure 1[13]).

The ciliary structure is also paramount for normal architecture and function of photoreceptors; hence, retinal dystrophy is an important manifestation of ciliopathies.[2,14,15] Nephrocystin 1 is expressed in photoreceptors and plays an important role in the intraflagellar transport between the inner and outer segments.[16,17] Therefore, *NPHP1* mutations are expected to result in retinal disease, a hypothesis supported by findings in a mouse model with a targeted disruption of *Nphp1*.[17–19] Hence, it is unexpected that visual impairment has previously only been reported in 20% to 23% of all patients affected by *NPHP1*-related NPH. A potential

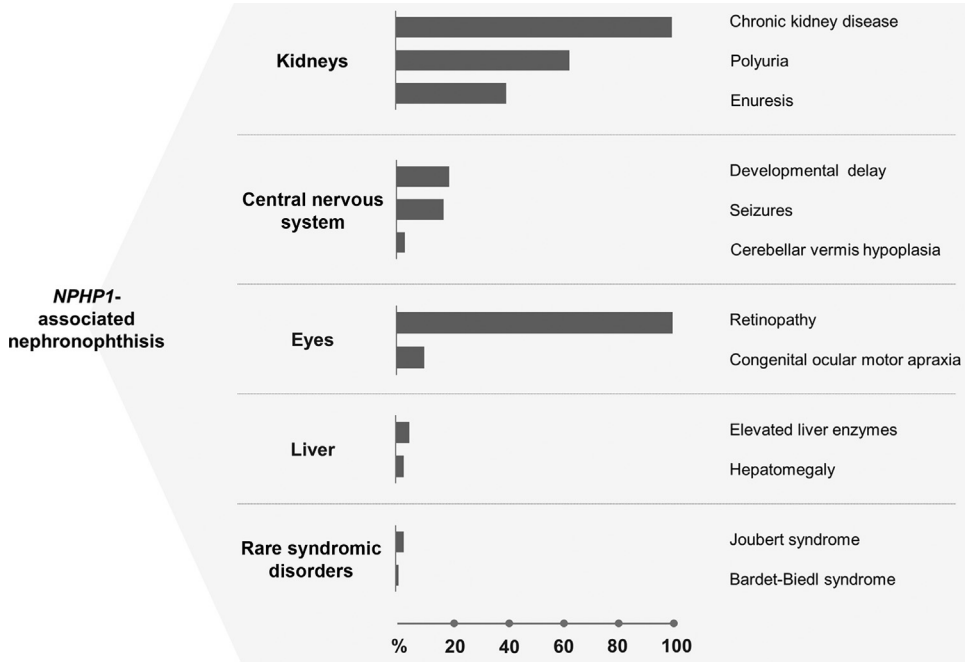


**Figure 1 | Spectrum of major disease manifestations in patients with *NPHP1*-associated nephronophthisis.** Frequencies are illustrated according to König *et al.*,[13] except for retinopathy, which is described in this report.

explanation could be that these reports have been based on patient records only and did not include in-depth retinal phenotyping.[13,20] The purpose of this study was an in-depth characterization of the retinal involvement in patients with nephronophthisis caused by homozygous *NPHP1* deletions.

## METHODS

### Patients

This retrospective, cross-sectional study was in adherence with the Declaration of Helsinki. Institutional review board approval and patients' informed consent were obtained. The study adhered to the Strengthening the Reporting of Observational Studies in Epidemiology guidelines.[21] All subjects were of Caucasian descent and were included in the network for early-onset cystic kidney diseases. The network for early-onset cystic kidney diseases is a multidisciplinary, multicenter collaboration that collects clinical data and addresses genetic, molecular, and functional questions of hereditary cystic kidney diseases.[22] A comprehensive general medical history was available for each patient, including nephrologic details such as disease onset, age at end-stage kidney disease,[23,24] dialysis and transplantation history, and nonrenal disease manifestations.

The inclusion criterion was the diagnosis of nephronophthisis due to variants in the *NPHP1* gene confirmed by genetic testing as part of the routine diagnostic workup[25–27] and retinal phenotyping. The exclusion criteria were any additional eye disease that may affect the patient's visual function and conditions preventing adequate image acquisition, such as significant opacities of the ocular media or very unstable fixation. In total, 16 patients were assessed and included in this multicenter and multidisciplinary study.

### Clinical ophthalmic examination and image acquisition

A precise history of visual symptoms was obtained, and a standardized clinical examination was performed. Clinical assessment included anterior segment and dilated fundus examination, best-corrected visual acuity testing, and full-field electroretinography (ERG) in accordance with the International Society for Clinical Electrophysiology of Vision standard[28] and color vision testing (saturated and desaturated Farnsworth D15). Visual field testing was performed using the 24-2 SITA-standard program of the Humphrey Field Analyzer (Zeiss) or the 30-2 SITA-standard program of the Oculus Twinfield Perimeter (Oculus). For quantification, the mean defect/mean deviation (MD) was used, representing the average difference between normal age-corrected sensitivity values and the measured threshold values at all test point locations. Discrete-level staging modified from the Hodapp-Parrish classification[29,30] was used to stage disease severity as mild (MD $< -6$ dB), moderate (MD $< -12$ dB), or advanced (MD $> -12$ dB) sensitivity loss.

Retinal imaging included spectral domain optical coherence tomography (OCT), fundus autofluorescence (AF) imaging (Spectralis HRA+OCT; Heidelberg Engineering), fundus photography (Visucam and Clarus, Zeiss), and in selected cases ultra-widefield pseudocolor and AF fundus imaging (Optos, Dunfermline, United Kingdom).[31,32]

Retinal thickness data were derived from OCT volume scans consisting of 61 horizontal B-scans (horizontal: 30°, vertical: 25°) with a distance of about 120 μm between individual scans and image averaging of ≥9 frames using the automated real-time mode. For detailed structural assessment, single scans through the foveal center with up to 100 averaged frames and thus better signal-to-noise ratio were also recorded. The Early Treatment Diabetic Retinopathy Study–type regions, with a subdivision of the central retina into 9 areas, was used for thickness measurements. The central region encompassed an area with a radius of 0.5 mm; the inner and outer rings were segmented into 4 quadrants, with radii of 1.5 and 3 mm, respectively. For comparison with healthy controls, normal reference values (mean in adults ± 2 standard deviations) were obtained from Chopovska *et al.*[33]

**Table 1 | Patient demographics and ophthalmologic findings**

| ID (#) | Symptoms (start of symptoms) | Age at (last) examination | Refraction (OD/OS) | BCVA (OD/S) | Nonretinal ophthalmic findings | Color vision testing | Visual field testing | MD dB (OD/OS) | ERG scotopic | ERG photopic |
|---|---|---|---|---|---|---|---|---|---|---|
| 1[a] | None | 6 | +2.50/−2.50/179°<br>+2.75/2.00/179° | 20/25<br>20/25 | None | NP | Not reliable due to reduced cooperation | — | NP | NP |
| 2 | None | 12 | +0.50/−3.00/12°<br>0.00/−4.00/166° | 20/25<br>20/20 | Oculomotor apraxia Cogan type in childhood | Normal | Not reliable due to fixation losses | — | NP | NP |
| 3 | None | 16 | −0.25/−1.00/10°<br>−0.50/−1.50/157° | 20/20<br>20/20 | Oculomotor apraxia Cogan type in childhood, strabismus | Normal | Minimal reduction of paracentral sensitivity | −2.6<br>−2.5 | Normal | Normal |
| 4 | None | 25 | −2.50/−1.00/118°<br>−3.00/−0.50/28° | 20/20<br>20/20 | None | Normal | Minimal reduction of paracentral sensitivity | −3.6<br>−2.9 | Normal | Normal |
| 5[b] | None | 21 | −1.50/−0.75/10°<br>+0.25/−1.00/20° | 20/20<br>20/20 | Strabismus surgery in childhood | Normal | Minimal reduction of paracentral sensitivity | −4.7<br>−3.0 | Normal | Normal |
| 6 | None | 32 | −5.50/−0.50/146°<br>−4.75/−2.25/59° | 20/20<br>20/20 | None | Normal | Minimal reduction of paracentral sensitivity | −3.4<br>−6.0 | Normal | Normal |
| 7[a] | None | 15 | 0.00/−1.00/18°<br>0.00/−1.25/11 | 20/20<br>20/20 | None | Normal | Minimal reduction of paracentral sensitivity | −3.3<br>−4.1 | Normal | Borderline reduced (80%) |
| 8 | Mild reduced night vision (not known) | 21 | −1.50/−1.50/4°<br>0.00/−1.25/3° | 20/20<br>20/20 | None | Minor confusions | Minimal reduction of paracentral sensitivity | −4.4<br>−2.6 | Normal | Borderline reduced (90%) |
| 9[b] | Mild increased glare (not known) | 23 | +5.50/−3.50/174°<br>+7.00/−5.00/4° | 20/25<br>20/25 | Strabismus surgery in childhood | Normal | Minimal reduction of paracentral sensitivity | −5.5<br>−5.2 | Normal | Borderline reduced (80%) |
| 10 | None | 13 | +1.75/−1.25/102°<br>+2.00/−1.75/76° | 20/20<br>20/20 | None | Normal | Minimal reduction of paracentral sensitivity | −6.6<br>−6.8 | NP | NP |
| 11 | Mild reduced night vision (childhood) | 15 | −0.75/−1.25/145°<br>−0.50/+1.50/1° | 20/20<br>20/20 | Oculomotor apraxia Cogan type in childhood with persisting minor problems | Normal | Minimal reduction of paracentral sensitivity | −6.9<br>−6.5 | Borderline reduced (90%) | Reduced (60%) |
| 12 | None | 17 | +2.25/−2.25/46°<br>+2.50/−1.75/136° | 20/20<br>20/20 | None | Normal | Global reduction of sensitivity in the central 30° | −11.5<br>−8.2 | NP | NP |
| 13 | Reduced night vision (childhood) | 12 | −0.75/−1.75/175°<br>+0.75/−2.25/156° | 20/32<br>20/40 | None | Normal | Minimal reduction of paracentral sensitivity | −4.9<br>−4.4 | Borderline reduced (90%) | Borderline reduced (80%) |
| 14 | Reduced night vision, mild increased glare (childhood) | 7 | −0.75/−0.75/10°<br>0.00/−1.25/147° | 20/32<br>20/32 | None | Abnormal | Paracentral scotoma | −19.0<br>−17.6 | Borderline reduced (90%) | Reduced (50%) |
| 15 | Reduced night vision (childhood) | 53 | +3.50/−1.50/127°<br>+3.00/−0.75/79° | 20/80<br>20/63 | None | Abnormal | Paracentral scotoma | −17.1<br>−15.2 | Reduced (50%) | Almost extinguished |
| 16 | Reduced night vision, mild increased glare, color vision abnormalities (childhood) | 28 | −6 dpt (OU) | 20/63<br>20/40 | Strabismus surgery in childhood, phakic intraocular lens at the age of 23 years | Abnormal | Paracentral scotoma | −19.7<br>−17.0 | Almost extinguished | Almost extinguished |

BCVA, best-corrected visual acuity; dpt, dioptre; ERG, full-field electroretinography; MD, mean defect/mean deviation; NP, not performed; OD, right eye; OS, left eye; OU, both eyes.
[a]Patients 1 and 7 are siblings.
[b]Patients 5 and 9 are siblings.
Color vision: in patient #2–#15 the desaturated Farnsworth D15 test was used, and in #16 the saturated test was used.

## RESULTS

The study included 16 patients from 14 families with an age at ophthalmic examination between 6 and 53 years (median, 17 years; interquartile range, 13–24 years; Table 1), all carrying a homozygous deletion of the entire *NPHP1* gene. Median best-corrected visual acuity was 20/20 (range, 20/80–20/20; interquartile range, 20/32–20/20); only the oldest patient (#15, 53 years old) and 1 further patient (#16) had a best-corrected visual acuity <20/40. Nine patients reported no vision problems, 6 were mildly symptomatic since childhood (4 with reduced night vision, 1 with glare, and 1 with reduced night vision and glare), and 1 patient had more severe vision problems (patient #16, see later). One patient had high hyperopia (patient #9), and 2 had boderline high myopia (patients #6 and #16); the remaining 13 patients had milder refractive errors (Table 1). In childhood, 3 patients had surgery for strabismus, and another 3 patients had Cogan-type oculomotor apraxia, which persisted in a mild form in 1 patient. No abnormalities of the anterior segment were found.

Overall, a high symmetry of the retinal phenotype between the right and left eye was identified; hence, retinal findings are reported for patients rather than for individual eyes. Fundoscopy in patients #1 through 15 revealed no obvious abnormalities in the central retina apart from an occasional faint granular appearance of the macula, whereas patient #16 exhibited advanced retinal degeneration (see later). None of the patients showed a coloboma or optic nerve atrophy. Central fundus AF images also appeared overall normal. However, OCT imaging consistently revealed distinct changes in the outer retinal layers, including a reduced reflectivity and often granular appearance of the ellipsoid zone line, fading or loss of the interdigitation zone, and narrowing of the distance between the ellipsoid zone and retinal pigment epithelium line, whereas the retinal pigment epithelium layer appeared to be preserved (Figure 2; Supplementary Figures S1–S3). The changes observed on OCT imaging were overall least pronounced or absent in the fovea. Retinal thickness maps revealed a (borderline) low retinal thickness outside the central sector of the fovea, which appeared to be mainly due to thinning of the photoreceptor layers (Figure 3). Ultra-widefield imaging was available from 8 patients, and no obvious abnormalities were observed in 6 patients. However, the oldest patient (53 years old) showed predominantly in the peripheral nasal retina bone spicule pigmentations corresponding to areas of reduced AF (Supplementary Figure S4). The retinal phenotype in the fundus periphery of patient #16 is described later.

Visual field testing was performed in all patients. The results of the 2 youngest patients were excluded from analysis because of poor reliability. Most patients (12 of 14) had a mild (mean MD = −3.9 dB; range, −2.5 to −6.0 dB; n = 8), moderate (MD = −6.7 dB, n = 1), or advanced (mean MD = −17.6 dB, n = 3) predominantly paracentral sensitivity loss, whereas the remaining 2 patients revealed a more global, diffuse reduction of sensitivity (MD = −6.7 dB and −9.9 dB). Color vision was tested in 15 patients and showed overall normal results in 12 cases and nonspecific abnormalities in 3 patients.

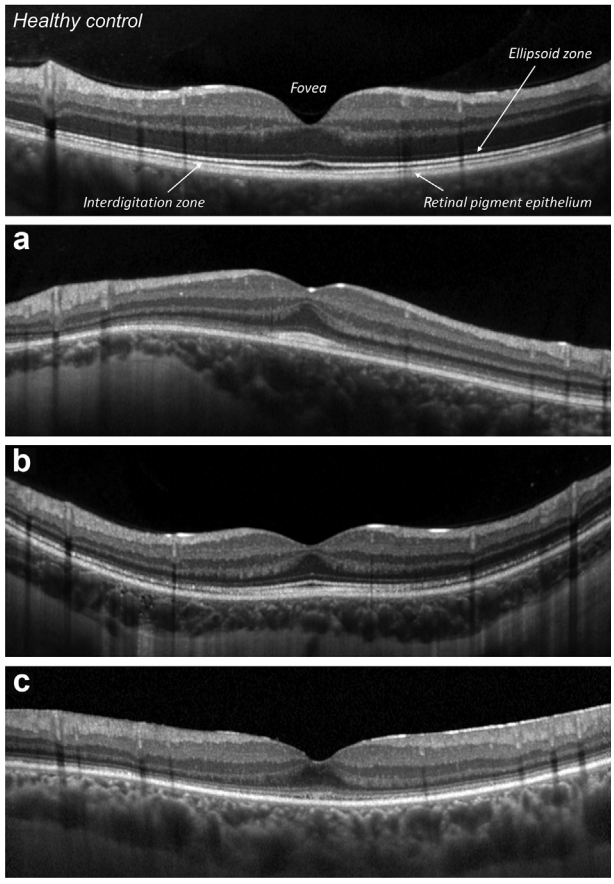


**Figure 2 | Optical coherence tomography of *NPHP1*-associated retinopathy.** There is a granular ellipsoid zone, fading of the interdigitation zone, and narrowing of the distance between the ellipsoid zone and the retinal pigment epithelium. Patients (**a**) #1, (**b**) #5, and (**c**) #15 are displayed.

Twelve patients underwent ERG testing. Scotopic amplitudes were within normal limits in the majority of the patients (7 of 12). The remaining 5 patients demonstrated a mild (80%–90% of the lower normal limit, n = 3), substantial (approximately 50% of the lower normal lower limit, n = 1), or nearly complete (n = 1) reduction of the scotopic amplitudes. Photopic amplitudes were within normal limits in 4 patients and otherwise showed a mild (80%–90% of the lower normal limit, n = 4), substantial (approximately 50% of the lower normal limit, n = 2), or nearly complete (n = 2) reduction. Overall, ERG testing indicated a mild cone or cone–rod dystrophy (Figure 4). The 3 patients (#14–#16) with the most severe retina-wide dysfunction on ERG testing also had the most advanced sensitivity losses on visual field testing and abnormal color vision.

As shown in Figure 5, the retinal phenotype of one 28-year-old patient (#16) differed from the mild retinal changes observed in all other 15 patients. He reported a progressive deterioration of visual function since childhood. Fundoscopy revealed a myopic fundus with pronounced

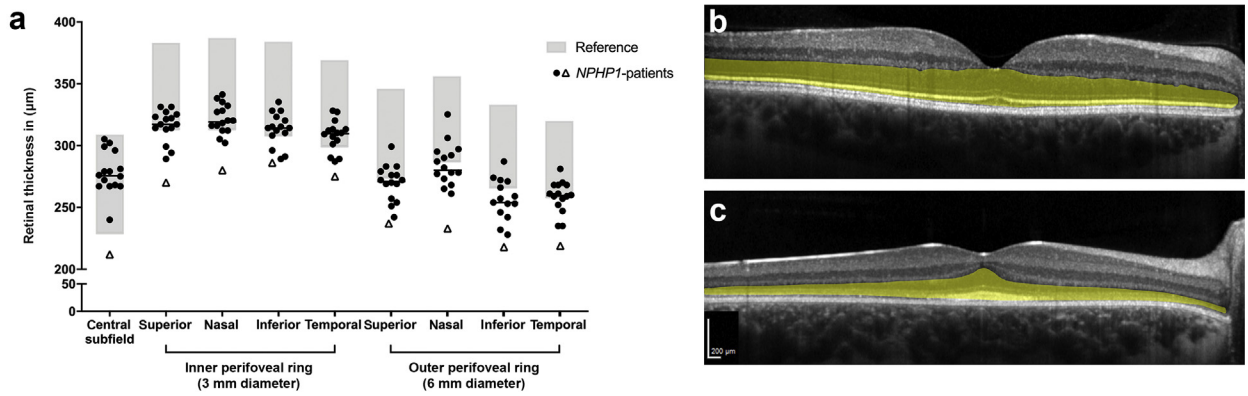


**Figure 3 | Subnormal retinal thickness in *NPHP1*-associated retinopathy.** (**a**) Retinal thickness mapping revealed (borderline) low macular thickness in *NPHP1*-associated retinopathy (dots) compared with healthy controls (mean ± 2 SD, gray bars), which appeared to be mainly due to thinning of the photoreceptor layers (**b**, control; **c,** patient 1; photoreceptor layers highlighted in yellow). Retinal thickness of patient #16 is indicated by triangles.

pigmentary changes and narrowing of retinal vessels. OCT imaging showed extensive photoreceptor loss with relative foveal sparing. Areas of reduced AF indicating advanced atrophic changes were located mainly at the eccentricity of the large arcades, with additional patchy areas of reduced AF more centrally. Photopic and scotopic full-field ERG amplitudes were almost extinguished, and a deep paracentral scotoma was visible on visual field testing. To assess a potential involvement of a second gene contributing to the more severe retinal alterations, further genetic investigations were performed. Copy number variations of the adjacent *MERTK* gene (~1.6 Mb distant from the *NPHP1* locus in the direction of the telomeric region [qtel] on the long arm of chromosome 2) were excluded by array comparative genomic hybridization (Supplementary Figure S5). Whole-exome sequencing identified a carrier state for another autosomal recessive ciliopathy, NPH type 6 (c. 4723A>T/p.[Lys1575*] in *NPHP6/CEP290*) and for achromatopsia type 3 (c.1208G>A/p.[Arg403Gln] in *CNGB3*).

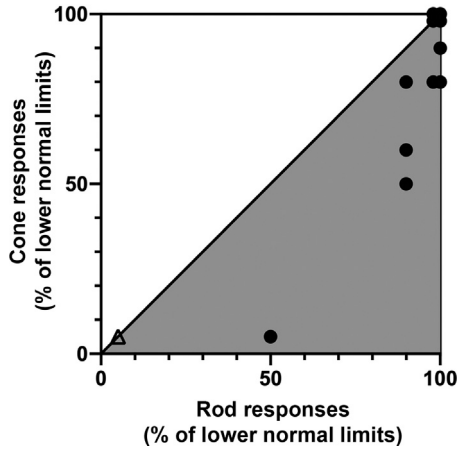


**Figure 4 | Predominant cone involvement on electrophysiology testing.** The relationship of rod and cone responses to the lower normal limits revealed a mild cone or cone–rod dystrophy in *NPHP1*-associated retinopathy. Oblique line, equal reduction of rod and cone amplitudes; gray area, greater cone than rod involvement; 100% lower normal limit, amplitudes within normal limits; dots, patients #3–#9, #11, and #13–#15; triangle, patient #16.

### Systemic disease associations

The diagnosis of nephronophthisis was established at a median age of 12 years (range, 1–32 years), with most patients presenting with a history of polyuria/polydipsia due to a urinary concentrating defect and/or clinical signs of advanced chronic kidney failure (Table 2[22,23]). In 1 asymptomatic patient (#1), preemptive diagnosis was established based on a family history of nephronophthisis. In 2 patients, genetic testing was initiated based on the ophthalmic presentation at the age of 1 (#11, oculomotor apraxia-type Cogan II) and 7 years (#14, deterioration of visual function and photophobia), respectively, with no obvious clinical signs of kidney disease at that time. Eight patients had received a kidney transplantation, which was performed at a median age of 15 years (range, 10–19 years). Before transplantation, 6 patients had received dialysis (median duration, 5 months; range, 1–24 months). At the time of assessment, 1 patient (#12) had been on dialysis for 21 months awaiting transplantation (Table 2). Besides the nephrologic and ophthalmologic findings, 5 patients revealed a multisystem involvement including ataxia (n = 3), developmental delay (n = 3), hypothyroidism (n = 1), and pancreatic neuroendocrine tumor (n = 1) (Table 2).

## DISCUSSION

We report a comprehensive in-depth ophthalmologic characterization of 16 patients with nephronophthisis caused by a homozygous deletion of the entire *NPHP1* gene. A distinct retinal phenotype on OCT imaging was identified, which typically remained without obvious correlates on clinical examination and AF imaging ("occult retinopathy"). Despite the predominant cone involvement on electrophysiology testing (mild cone or cone–rod dystrophy in more advanced cases), night vision problems were reported as an early symptom, and degenerative changes show a relative sparing of the fovea. So far, *NPHP1*-associated retinopathy may have

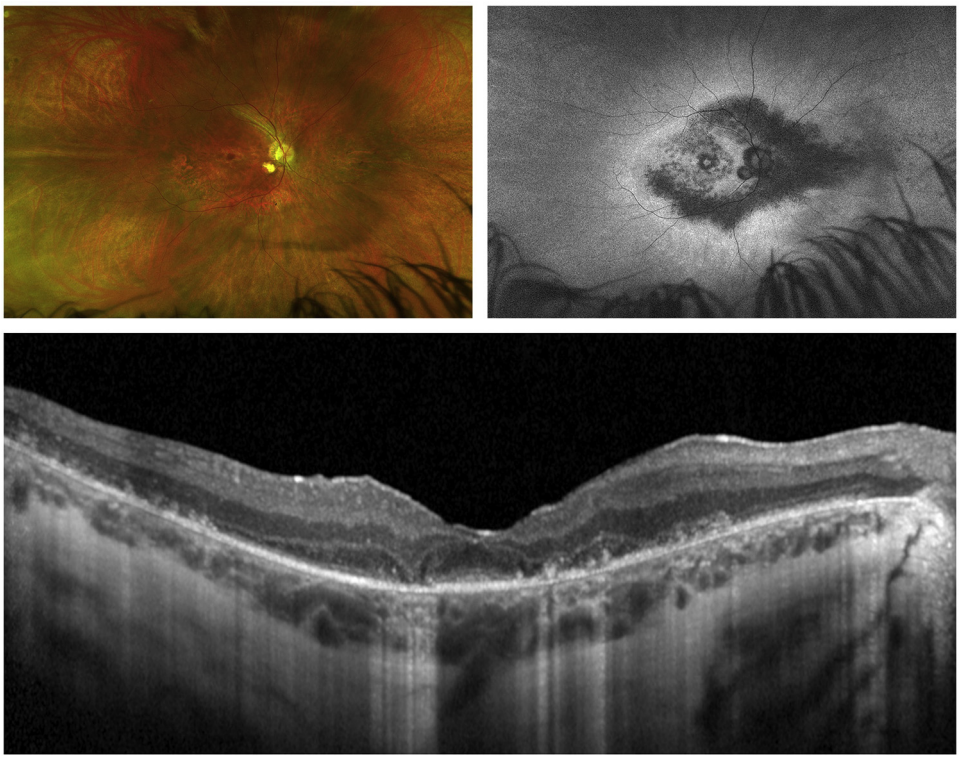

**Figure 5 | Retinal phenotype of *NPHP1*-associated retinopathy—patient #16.** Widefield false-color image (top left), widefield fundus autofluorescence (top right), and optical coherence tomography (bottom) images.

been underreported because of the usually mild structural changes or, when diagnosed, misinterpreted as retinitis pigmentosa, characterized by a rod instead of cone-dominated dysfunction in patients with reduced night vision.

In patients with occult retinopathy, consistent features on OCT imaging included reduced reflectivity of the ellipsoid zone, fading or absence of the interdigitation zone, and narrowing of the distance between the ellipsoid zone and the retinal pigment

**Table 2 | Kidney function and kidney transplantation history**

| ID (#) | Sex, M/F | Serum creatinine level at evaluation, mg/dl | eGFR at evaluation, ml/min per 1.73 $m^2$ | Chronic kidney disease stage | Age at diagnosis nephronophthisis, yr | Age at end-stage kidney failure, yr | Age at kidney transplantation, yr | Extrarenal disease |
|---|---|---|---|---|---|---|---|---|
| 1 | M | 0.43 | 112 | I | 2 | — | — | — |
| 2 | M | 1.9 | 32.8 | III | 9 | 10 | 10 | Hypothyroidism |
| 3 | M | 0.7 | 138.2 | I | 1 | 10 | 10 | Oculomotor apraxia, ataxia, developmental delay |
| 4 | M | 2.4 | 36.3 | III | 21 | 24 | 25 | — |
| 5 | M | 2.9 | 30.0 | III | 17 | — | — | — |
| 6 | F | 5.5 | 9.5 | V | 32 | 32 | — | Pancreatic neuroendocrine tumor |
| 7 | F | 1.9 | 38.8 | III | 11 | 11 | 11 | — |
| 8 | M | 1.5 | 65.6 | II | 15 | 15 | 16 | — |
| 9 | M | 1.9 | 48 | III | 18 | 18 | 19 | — |
| 10 | M | 3.1 | 26.3 | IV | 12 | — | — | — |
| 11 | M | 1.7 | 53.4 | III | 6 | — | — | Ataxia, language, and motor developmental delay |
| 12 | M | 7.7 | 11 | V | 14 | 15 | 18 | Ataxia, developmental delay |
| 13 | M | 3.2 | 23.8 | IV | 9 | 12 | 13 | — |
| 14 | M | 1.0 | 70.0 | II | 7 | — | — | — |
| 15 | F | NE | NE | NE | 12 | 14 | NE | — |
| 16 | M | 4 | 19.1 | IV | 27 | 29 | 29 | — |

eGFR, estimated glomerular filtration rate; F, female; M, male; NE, not evaluated around the time of ophthalmic examination.
End-stage kidney failure defined as previously classified.[22,23]

epithelium, but preservation of the retinal pigment epithelium. Retinal thickness is often mildly reduced, and the fovea remains relatively spared. These structural alterations of the retina are similar to changes observed in patients with *POC1B*-associated ciliopathy. However, *POC1B*-associated retinopathy seems to present with more severe loss of cone function on ERG testing and little or no rod dysfunction (also described as a "peripheral cone dystrophy" because of the relative foveal sparing).[34–37] Occult macular dystrophy due to variants in the *RP1L1* gene is another disease with similar phenotypic features, although the structural and functional changes primarily affect the fovea.[38–41] The gene products of *NPHP1*, *POC1B*, and *RP1L1* play a role in ciliary structure and function. The phenotypic similarity may define a distinct group of occult cone-dominant retinal ciliopathies with similar pathophysiology, apparently with a gene-specific topographic distribution of cone involvement and possible additional rod dysfunction.[35–41] Different phenotypic features have been reported in other retinal ciliopathies that may predominantly affect cones, such as *RPGR*- or *KIF11*-associated cone–rod dystrophy, indicating different disease mechanisms.[15,42]

In *Nphp1* gene-trap mutant mice, which are likely hypomorphs due to the production of a small quantity of functional messenger RNAs, photoreceptors fail to develop normal outer segments because of an impaired intraflagellar transport.[16,17,19] Such abnormal photoreceptor outer segments are likely the structural correlate for the consistent human phenotype on OCT imaging that is already present in very mild disease (see earlier). Over time, the mouse model develops photoreceptor atrophy, which again finds its OCT-based correlate in thinning of the outer retina in humans.[17] Hence, the mouse model with a targeted disruption of *Nphp1* recapitulates *NPHP1*-associated retinopathy in humans and may be used for preclinical evaluation of novel therapies. Indeed, *NPHP1*-associated retinopathy is an ideal candidate for gene therapy because the 3.8-kb complementary DNA can be packaged into adeno-associated viral vectors, which have been established as a safe and efficient vector for retinal gene therapy.[43]

Profound vision-related disease burden would be a rationale for developing therapeutic approaches. In this cohort, the oldest patient had moderate vision loss at the age of 53 years, no other patient was over 35 years of age, and the individual with the second most severely affected ERG responses was only 7 years old. If the severity of *NPHP1*-associated retinopathy is heterogenous with severe vision loss in some older patients, this may have been missed in this cross-sectional study because of the small sample size of mostly younger individuals. Whether (some) patients eventually develop an almost complete photoreceptor atrophy in line with findings in the 8-month-old mouse model remains unclear and is subject to further investigations.

Previous studies identified a retinal involvement in only 20% to 23% of patients with juvenile nephronophthisis caused by *NPHP1* variants,[13,20] whereas retinal alterations were seen in all 16 pediatric and adult patients in our study. This discrepancy is likely explained by underreporting in earlier studies that did not include in-depth phenotyping. A similarly benign phenotype in patients with *NPHP1*-related Joubert syndrome[44,45] indicates that *NPHP1*-associated retinopathy is mostly mild, independent from systemic disease manifestations. Of note, reduced night vision as an early symptom may have caused misconceptions concerning the retinal involvement because this symptom is frequently, but not exclusively, present in rod-cone dystrophy (retinitis pigmentosa). The study by Caridi *et al.*[46] is frequently referenced for an association of nephronophthisis and retinitis pigmentosa. However, they explicitly mentioned that *NPHP1*-associated disease is "distinct from the classical Senior-Løken syndrome," which presents with retinitis pigmentosa.[46]

Future deep phenotyping with multimodal retinal imaging in all NPH patients may disclose whether different NPH genotypes are associated with specific retinal phenotypes. This would potentially allow more precise and reliable patient counseling regarding long-term visual prognosis. Moreover, detailed retinal assessment could then be helpful in the differential diagnosis of NPH patients, and specific retinal findings could alert clinicians to investigate the patient's kidneys. Of note, patient #14 in our cohort was diagnosed based on the retinal changes, and subsequent genetic testing had a major impact on clinical management and renal prognosis. Therefore, detailed retinal phenotyping can guide the diagnosis of NPH, which is important because underdiagnosis of *NPHP1*-related disease is common, even when extrarenal anomalies are present.[47,48]

Compared with the milder occult retinopathy in all other 15 patients, 1 patient (#16) had more severe retinal degeneration. He carried an additional pathogenic variant in another ciliopathy gene, *CEP290*, and a likely pathogenic, but at the most hypomorphic, *CNGB3* variant. *CEP290* encodes for nephrocystin-6, a protein located in the interconnecting cilium where it interacts with many ciliary proteins, including the NPHP complex, RPGR, and AHI1.[49–53] The presence of a heterozygous variant in *Cep290* has been reported to result in more rapid retinal degeneration in mice lacking *Rpgr*, and variants in *Ahi1/AHI1* have been reported to modify *Nphp1*- (in mice) as well as *CEP290*-related retinal degeneration (in humans).[52–54] Recently, Datta *et al.*[19] demonstrated that a reduced gene dose of *Cep290* exacerbates protein mislocalization and retinal degeneration in *Nphp1* mutant mice. Furthermore, it has been shown that *CEP290* variants can modify the extrarenal symptoms in patients with *NPHP1* mutations,[45] a phenomenon also seen in other ciliopathies such as Bardet-Biedl syndrome. Hence, one can speculate that the *CEP290* variant might act as a genetic modifier of *NPHP1*-related retinopathy, resulting in more severe retinal degeneration.

We found 2 previous reports that included a detailed illustration of the retinal phenotype in patients with *NPHP1*-associated nephronophthisis ($n_{total} = 7$).[55,56] At least some of these patients had a rather advanced retinal degeneration at a younger age, similar to the severely affected patient #16 of this study. It remains unclear if this is a subgroup of patients that

was referred to an ophthalmologist because they reported reduced vision, which would result in a selection bias favoring a more severe retinal phenotype. It also remains unclear if these patients were also carriers for variants in other ciliopathy/retinal dystrophy genes that might act as genetic modifiers. Furthermore, pronounced retinal degeneration might be present at an older age, as suggested by the peripheral changes observed in the oldest patient of our cohort.

This study is limited by its retrospective design, the relatively small number of included patients, an intrinsic challenge of reporting phenotypic findings in rare diseases, and a lack of longitudinal observation periods. It also remains to be investigated if our findings also apply to patients with late-onset nephronophthisis and if juvenile nephronophthisis patients show more advanced retinal alterations at an older age. The usually well-preserved visual acuity and predominantly paracentral visual field loss found in this study indicate good functional correlation with structural alterations on OCT imaging (relative foveal sparing). However, this may need to be further investigated in future studies that include microperimetry and multifocal ERG testing.

In summary, this study illustrates a distinct retinal phenotype on OCT imaging without obvious correlates on clinical examination and AF imaging. Diagnostic awareness about this ciliopathy that predominantly affects cones may assist in the differential diagnosis of nephronophthisis and for individual prognosis of visual function. More advanced retinal degeneration may occur due to aging and possibly due to genetic modifiers (here an additional *CEP290* variant).

## DISCLOSURE

All the authors declared no competing interests.

## ACKNOWLEDGMENTS

This work was supported by the Dr. Werner Jackstädt Foundation, Wuppertal, Germany (grant S0134-10.22 to JB), the Bayer Global Ophthalmology Awards Program (to JB), and the National Institute for Health Research (NIHR) Oxford Biomedical Research Centre (BRC). As a part of the Neocyst consortium, this study was funded by the German Federal Ministry of Research and Education (BMBF, grant 01GM1903A). The funding organizations had no role in the design and conduct of the study; collection, management, analysis, and interpretation of the data; preparation, review, or approval of the manuscript; and decision to submit the manuscript for publication. The views expressed are those of the authors and not necessarily those of the NHS, the National Institute of Health, or the Department of Health.

## SUPPLEMENTARY MATERIAL

Supplementary File (PDF)

**Figure S1.** Retinal phenotype of *NPHP1*-associated retinopathy—control and patients #1–#5. Fundus autofluorescence (AF) and optical coherence tomography (OCT) of a healthy control (top row) and of patients with *NPHP1*-associated retinopathy (#1–#5). Only 1 eye is shown per patient due to high symmetry between eyes.

**Figure S2.** Retinal phenotype of *NPHP1*-associated retinopathy—patients #6–#11. Fundus autofluorescence (AF) and optical coherence tomography (OCT) images of patients with *NPHP1*-associated retinopathy (#6–#11). Only 1 eye is shown per patient due to high symmetry between eyes.

**Figure S3.** Retinal phenotype of *NPHP1*-associated retinopathy—patients #12–#15. Fundus autofluorescence (left) and optical coherence tomography (right) images of patients with *NPHP1*-associated retinopathy (#12–#15) are displayed. Only 1 eye is shown per patient due to high symmetry between eyes.

**Figure S4.** Ultra-widefield pseudo-color (first row) and fundus autofluorescence (second row) images of the right and left eye of patient #15.

**Figure S5.** Synopsis of array comparative genomic hybridization (CGH, **A,B**) and multiplex ligation-dependent probe amplification (MLPA, **C**) analyses of patient #16. Array CGH and MLPA analyses confirmed homozygous *NPHP1* gene deletion identified previously from NGS sequencing data. (**A**) Idiogram of human chromosome 2 with region of interest marked in blue for general orientation (upper panel) and copy number analysis by array CGH of the respective section (lower panel) depicting the two different *NPHP1* deletion alleles: 1 larger deletion approximately 290 kb (the typical deletion size identified by reference 12) and 1 smaller deletion approximately 155 kb in size (*nota bene* assignment of heterozygous-deleted genomic regions outside of *NPHP1* to both alleles is arbitrary in the absence of parental segregation). Both deletions do not include the *MERTK* gene (associated with autosomal recessive retinitis pigment type 38) located ca. 1.6 Mb apart in telomeric direction on the long arm (qtel). (Centromere marked with cen and telomere end of the short arm marked with ptel). (**B**) Array CGH enlargement with detailed view on *NPHP1* locus (lower panel) and schematic integration with the flanking 330 kb (330RI/II) and 45 kb (45RI/II) low copy number repeats marked in blue and green (upper panel, modified from reference 12). (**C**) Shows (exemplary) MLPA findings on DNA of patient #16. Amplification of the patient DNA (in green) compared with male control DNA samples (in blue) for specific DNA fragments on the X and Y chromosome and for *NPHP1* exon 1 to 20 yields no signal for all *NPHP1* exons. Quantitative assessment of exon-specific probe amplification is commonly performed for targeted testing or reconfirmation of *NPHP1*-associated nephronophthisis using the commercial MLPA-probe mix P387-A3 from MRC Holland (Amsterdam, The Netherlands; containing probes for all *NPHP1* exons, spanning approximately 82.7 kb of genomic DNA). MLPA findings depicted with the MLPA module of the Sequence Pilot software (JSI Medical Systems).

## REFERENCES

1. Wolf MT. Nephronophthisis and related syndromes. *Curr Opin Pediatr*. 2015;27:201–211.
2. Hildebrandt F, Benzing T, Katsanis N. Ciliopathies. *N Engl J Med*. 2011;364:1533–1543.
3. Hildebrandt F, Nothwang HG, Vossmerbaumer U, et al. Lack of large, homozygous deletions of the nephronophthisis 1 region in Joubert syndrome type B. APN Study Group. Arbeitsgemeinschaft fur Padiatrische Nephrologie. *Pediatr Nephrol*. 1998;12:16–19.
4. Srivastava S, Molinari E, Raman S, et al. Many genes-one disease? Genetics of nephronophthisis (NPHP) and NPHP-associated disorders. *Front Pediatr*. 2017;5:287.
5. Gusmano R, Ghiggeri GM, Caridi G. Nephronophthisis-medullary cystic disease: clinical and genetic aspects. *J Nephrol*. 1998;11:224–228.
6. Salomon R, Saunier S, Niaudet P. Nephronophthisis. *Pediatr Nephrol*. 2009;24:2333–2344.
7. Halbritter J, Porath JD, Diaz KA, et al. Identification of 99 novel mutations in a worldwide cohort of 1,056 patients with a nephronophthisis-related ciliopathy. *Hum Genet*. 2013;132:865–884.
8. Hildebrandt F, Otto E, Rensing C, et al. A novel gene encoding an SH3 domain protein is mutated in nephronophthisis type 1. *Nat Genet*. 1997;17:149–153.
9. Antignac C, Arduy CH, Beckmann JS, et al. A gene for familial juvenile nephronophthisis (recessive medullary cystic kidney disease) maps to chromosome 2p. *Nat Genet*. 1993;3:342–345.

10. Konrad M, Saunier S, Heidet L, et al. Large homozygous deletions of the 2q13 region are a major cause of juvenile nephronophthisis. *Hum Mol Genet*. 1996;5:367–371.
11. Saunier S, Calado J, Benessy F, et al. Characterization of the NPHP1 locus: mutational mechanism involved in deletions in familial juvenile nephronophthisis. *Am J Hum Genet*. 2000;66:778–789.
12. Fliegauf M, Benzing T, Omran H. When cilia go bad: cilia defects and ciliopathies. *Nat Rev Mol Cell Biol*. 2007;8:880–893.
13. König J, Kranz B, König S, et al. Phenotypic spectrum of children with nephronophthisis and related ciliopathies. *Clin J Am Soc Nephrol*. 2017;12:1974–1983.
14. May-Simera H, Nagel-Wolfrum K, Wolfrum U. Cilia - the sensory antennae in the eye. *Prog Retin Eye Res*. 2017;60:144–180.
15. Birtel J, Gliem M, Mangold E, et al. Novel insights into the phenotypical spectrum of KIF11-associated retinopathy, including a new form of retinal ciliopathy. *Invest Ophthalmol Vis Sci*. 2017;58:3950–3959.
16. Fliegauf M, Horvath J, von Schnakenburg C, et al. Nephrocystin specifically localizes to the transition zone of renal and respiratory cilia and photoreceptor connecting cilia. *J Am Soc Nephrol*. 2006;17:2424–2433.
17. Jiang ST, Chiou YY, Wang E, et al. Essential role of nephrocystin in photoreceptor intraflagellar transport in mouse. *Hum Mol Genet*. 2009;18:1566–1577.
18. Jiang ST, Chiou YY, Wang E, et al. Targeted disruption of Nphp1 causes male infertility due to defects in the later steps of sperm morphogenesis in mice. *Hum Mol Genet*. 2008;17:3368–3379.
19. Datta P, Cribbs JT, Seo S. Differential requirement of NPHP1 for compartmentalized protein localization during photoreceptor outer segment development and maintenance. *PLoS One*. 2021;16:e0246358.
20. Soliman NA, Hildebrandt F, Otto EA, et al. Clinical characterization and NPHP1 mutations in nephronophthisis and associated ciliopathies: a single center experience. *Saudi J Kidney Dis Transpl*. 2012;23:1090–1098.
21. von Elm E, Altman DG, Egger M, et al. The Strengthening the Reporting of Observational Studies in Epidemiology (STROBE) statement: guidelines for reporting observational studies. *Lancet*. 2007;370:1453–1457.
22. König JC, Titieni A, Konrad M, et al. Network for early onset cystic kidney diseases-a comprehensive multidisciplinary approach to hereditary cystic kidney diseases in childhood. *Front Pediatr*. 2018;6:24.
23. Hogg RJ, Furth S, Lemley KV, et al. National Kidney Foundation's Kidney Disease Outcomes Quality Initiative clinical practice guidelines for chronic kidney disease in children and adolescents: evaluation, classification, and stratification. *Pediatrics*. 2003;111:1416–1421.
24. Stevens PE, Levin A, Kidney Disease: Improving Global Outcomes Chronic Kidney Disease Guideline Development Work Group Members. Evaluation and management of chronic kidney disease: synopsis of the kidney disease: improving global outcomes 2012 clinical practice guideline. *Ann Intern Med*. 2013;158:825–830.
25. Hildebrandt F, Rensing C, Betz R, et al. Establishing an algorithm for molecular genetic diagnostics in 127 families with juvenile nephronophthisis. *Kidney Int*. 2001;59:434–445.
26. Birtel J, Eisenberger T, Gliem M, et al. Clinical and genetic characteristics of 251 consecutive patients with macular and cone/cone-rod dystrophy. *Sci Rep*. 2018;8:4824.
27. Javorszky E, Moriniere V, Kerti A, et al. QMPSF is sensitive and specific in the detection of NPHP1 heterozygous deletions. *Clin Chem Lab Med*. 2017;55:809–816.
28. McCulloch DL, Marmor MF, Brigell MG, et al. ISCEV Standard for full-field clinical electroretinography (2015 update). *Doc Ophthalmol*. 2015;130:1–12.
29. Hodapp E, Parrish RK, Anderson DR. *Clinical Decisions in Glaucoma*. St Louis, MO: Mosby; 1993.
30. Mills RP, Budenz DL, Lee PP, et al. Categorizing the stage of glaucoma from pre-diagnosis to end-stage disease. *Am J Ophthalmol*. 2006;141:24–30.
31. Birtel J, Gliem M, Holz FG, et al. [Imaging and molecular genetic diagnostics for the characterization of retinal dystrophies]. *Ophthalmologe*. 2018;115:1021–1027.
32. Birtel J, Yusuf IH, Priglinger C, et al. Diagnosis of inherited retinal diseases. *Klin Monbl Augenheilkd*. 2021;238:249–260.
33. Chopovska Y, Jaeger M, Rambow R, et al. Comparison of central retinal thickness in healthy children and adults measured with the Heidelberg Spectralis OCT and the zeiss Stratus OCT 3. *Ophthalmologica*. 2011;225:27–36.
34. Jin X, Chen L, Wang D, et al. Novel compound heterozygous mutation in the POC1B gene underlie peripheral cone dystrophy in a Chinese family. *Ophthalmic Genet*. 2018;39:300–306.
35. Kameya S, Fujinami K, Ueno S, et al. Phenotypical characteristics of POC1B-associated retinopathy in Japanese cohort: cone dystrophy with normal funduscopic appearance. *Invest Ophthalmol Vis Sci*. 2019;60:3432–3446.
36. Kondo M, Miyake Y, Kondo N, et al. Peripheral cone dystrophy: a variant of cone dystrophy with predominant dysfunction in the peripheral cone system. *Ophthalmology*. 2004;111:732–739.
37. Durlu YK, Koroglu C, Tolun A. Novel recessive cone-rod dystrophy caused by POC1B mutation. *JAMA Ophthalmol*. 2014;132:1185–1191.
38. Akahori M, Tsunoda K, Miyake Y, et al. Dominant mutations in RP1L1 are responsible for occult macular dystrophy. *Am J Hum Genet*. 2010;87:424–429.
39. Nakamura N, Tsunoda K, Mizuno Y, et al. Clinical stages of occult macular dystrophy based on optical coherence tomographic findings. *Invest Ophthalmol Vis Sci*. 2019;60:4691–4700.
40. Davidson AE, Sergouniotis PI, Mackay DS, et al. RP1L1 variants are associated with a spectrum of inherited retinal diseases including retinitis pigmentosa and occult macular dystrophy. *Hum Mutat*. 2013;34:506–514.
41. Miyake Y, Ichikawa K, Shiose Y, et al. Hereditary macular dystrophy without visible fundus abnormality. *Am J Ophthalmol*. 1989;108:292–299.
42. Hong DH, Pawlyk B, Sokolov M, et al. RPGR isoforms in photoreceptor connecting cilia and the transitional zone of motile cilia. *Invest Ophthalmol Vis Sci*. 2003;44:2413–2421.
43. Lipinski DM, Thake M, MacLaren RE. Clinical applications of retinal gene therapy. *Prog Retin Eye Res*. 2013;32:22–47.
44. Brooks BP, Zein WM, Thompson AH, et al. Joubert syndrome: ophthalmological findings in correlation with genotype and hepatorenal disease in 99 patients prospectively evaluated at a single center. *Ophthalmology*. 2018;125:1937–1952.
45. Tory K, Lacoste T, Burglen L, et al. High NPHP1 and NPHP6 mutation rate in patients with Joubert syndrome and nephronophthisis: potential epistatic effect of NPHP6 and AHI1 mutations in patients with NPHP1 mutations. *J Am Soc Nephrol*. 2007;18:1566–1575.
46. Caridi G, Murer L, Bellantuono R, et al. Renal-retinal syndromes: association of retinal anomalies and recessive nephronophthisis in patients with homozygous deletion of the NPH1 locus. *Am J Kidney Dis*. 1998;32:1059–1062.
47. Hoefele J, Nayir A, Chaki M, et al. Pseudodominant inheritance of nephronophthisis caused by a homozygous NPHP1 deletion. *Pediatr Nephrol*. 2011;26:967–971.
48. Snoek R, van Setten J, Keating BJ, et al. NPHP1 (nephrocystin-1) gene deletions cause adult-onset ESRD. *J Am Soc Nephrol*. 2018;29:1772–1779.
49. Badano JL, Leitch CC, Ansley SJ, et al. Dissection of epistasis in oligogenic Bardet-Biedl syndrome. *Nature*. 2006;439:326–330.
50. Fahim AT, Bowne SJ, Sullivan LS, et al. Polymorphic variation of RPGRIP1L and IQCB1 as modifiers of X-linked retinitis pigmentosa caused by mutations in RPGR. *Adv Exp Med Biol*. 2012;723:313–320.
51. Badano JL, Kim JC, Hoskins BE, et al. Heterozygous mutations in BBS1, BBS2 and BBS6 have a potential epistatic effect on Bardet-Biedl patients with two mutations at a second BBS locus. *Hum Mol Genet*. 2003;12:1651–1659.
52. Coppieters F, Casteels I, Meire F, et al. Genetic screening of LCA in Belgium: predominance of CEP290 and identification of potential modifier alleles in AHI1 of CEP290-related phenotypes. *Hum Mutat*. 2010;31:E1709–E1766.
53. Rao KN, Zhang W, Li L, et al. Ciliopathy-associated protein CEP290 modifies the severity of retinal degeneration due to loss of RPGR. *Hum Mol Genet*. 2016;25:2005–2012.
54. Louie CM, Caridi G, Lopes VS, et al. AHI1 is required for photoreceptor outer segment development and is a modifier for retinal degeneration in nephronophthisis. *Nat Genet*. 2010;42:175–180.
55. Yahalom C, Volovelsky O, Macarov M, et al. Senior-Løken syndrome: a case series and review of the reno-retinal phenotype and advances of molecular diagnosis. *Retina*. 2021;41:2179–2187.
56. Kang HG, Ahn YH, Kim JH, et al. Atypical retinopathy in patients with nephronophthisis type 1: an uncommon ophthalmological finding. *Clin Exp Ophthalmol*. 2015;43:437–442.